Three-photon frequency down-conversion as an event-ready source of entangled states

Alejandro A. Hnilo*
Centro de Investigaciones en Laseres y Aplicaciones (CEILAP) (CITEFA-CONICET-UNSAM),
Instituto de Investigaciones Científicas y Técnicas de las FFAA (CITEFA),
Consejo Nacional de Investigaciones Científicas y Tecnológicas (CONICET),
Universidad Nacional de San Martín (UNSAM), Argentina
(Received 2 November 2004; published 31 March 2005)

An event-ready (or deterministic) source of entangled states is of interest in the practical implementation of schemes of quantum computation and cryptography as well as in the experiments aimed to elucidate the foundations of quantum mechanics. I study the phase matching geometry and detection conditions for the process of three-photon frequency down-conversion, which is a possible source of that kind. It is apparently free of some limitations of the schemes based on two-photon frequency down-conversion. The goal of the proposed setup is not the generation of an entangled state of three photons (in a GHZ-state sense), but of an entangled state of two photons with a "trigger" signal. As an example, I estimate the values of the trios' flux and trigger's reliability for the particular case of crystal calcite illuminated by the fourth harmonic of a Nd:YAG mode-locked laser.

DOI: 10.1103/PhysRevA.71.033820 PACS number(s): 42.65.Lm, 03.65.Ud, 42.50.Dv, 03.67.−a

I. INTRODUCTION

Practical sources of entangled states of two photons (or "biphotons") are of obvious interest for schemes of quantum computation and communications. Many theoretical studies of these schemes naturally assume that the entangled states can be produced at will—i.e., in a *deterministic* way [1]. The most widespread sources of biphotons are based on the two-photon frequency down-conversion process (2PDC) of near-UV laser radiation in a nonlinear crystal [2]. But the state these sources produce is of the form

$$|0\rangle + \xi|\phi\rangle + o(\xi^2), \tag{1}$$

where the first term corresponds to the vacuum state of the field, $|\phi\rangle$ is one of the Bell states, and $|\xi| \ll 1$. As one cannot ensure that an entangled state will be detected (even if a perfect detector were available) when (1) is observed, this kind of source has been named *random* source of entangled states [1]. Besides being undesirable for the applications mentioned above, states described by Eq. (1) cannot produce a violation of Bell's inequalities free of one of several possible logical loopholes (to mention just a few: the *no-enhancement* or *fair sampling* assumption [3], Scalera's counterexample [4], and the *no-trapping* assumption [5]), even if perfect collecting optics and detectors were available. In studies of this subject, "deterministic" sources are also named "event-ready" sources, and they have been known to be essential since Bell's early contributions [6].

Among the efforts made to achieve a deterministic source of biphotons should be noted the scheme proposed by Zukowski *et al.* [7] and realized, among others, by Pan *et al.* [8]. It is based on a double passage of an ultrashort laser pulse through a nonlinear crystal, so that *two* processes of two-photon frequency down-conversion (2PDC) occur. The probability of the generation of one pair on each passage $|\xi|^2$ is small in practice, so that the total rate of event-ready biphotons (which is equal to the fourfold coincidence rate) is very low, on the order of a few hundred in several hours. Even though these numbers can show some improvement by increasing the power of the incident UV radiation, a low rate is inescapable. For the probability of generating one pair, in each of the 2PDC processes, must be kept small in order to reduce, to negligible levels, the probability of the generation of *two* pairs on each passage. Otherwise, the entanglement would be spoiled. Therefore, one is faced with the problem that the signal (which comes from two 2PDC processes) is of the same order as the noise (which comes, among other sources, from two 2PDC processes too). A general argument has been presented [1] claiming that Bell states with maximal entanglement cannot be generated in setups based on two 2PDC processes. It has been theoretically demonstrated that a setup based on *three* 2PDC processes, where the biphoton is heralded by four trigger photons, is able to prepare a maximally entangled state [9]. But, of course, the rate of biphotons would be even lower than in two 2PDC.

At this point, it is natural to explore the feasibility of processes based on three-photon frequency down-conversion (3PDC). This possibility has been generally discarded, because the available third-order susceptibility is much smaller than the second-order one, and hence the generated fluorescence is extremely faint. However, as is shown later, the rate of event-ready biphotons is comparable with what can be obtained from two 2PDC processes, and there is no apparent limitations on the purity of the entanglement.

The 3PDC process has been theoretically studied as a source of nonclassical field states both in parametric oscillator cavities and in running wave configurations, but only in the collinear and degenerate case. To my knowledge, there are no published studies of the conditions for noncollinear phase matching. In this paper, I calculate these conditions and also study the feasibility of using 3PDC as a determin-

*Permanent address: CITEFA; J.B. de La Salle 4397, B1603ALO Villa Martelli, Argentina. Electronic address: ahnilo@citefa.gov.ar

istic or event-ready source of entangled states. It is important to note from the beginning that I am not seeking a three-photon entangled state in the sense of the Greenberger-Horne-Zeilinger states, but for a state of the general form

$$|0\rangle + \xi(|t_3\rangle \otimes |\phi_{12}\rangle + |\perp t_3\rangle \otimes \cdots) + o(\xi^2), \tag{2}$$

where $|\phi_{12}\rangle$ is a Bell state of photons 1 and 2, $|t_3\rangle$ is any pure state of photon 3, and $|\perp t_3\rangle$ represents the states orthogonal to $|t_3\rangle$. In this way, one is sure that if $|t_3\rangle$ (the "trigger" or "event-ready" signal) is detected on photon 3, then a Bell state is available on photons 1 and 2.

In the next section, I review the basics of the 3PDC process. The only important difference from the 2PDC case is in the phase-matching conditions. I describe a possible setup in Sec. III. The problem of collecting and focusing the frequency down-converted radiation is the main technical obstacle that determines how close to an ideal source it is possible to go. In the last section, I present a calculation of the performance that can be expected in practice, in the particular case of a calcite crystal illuminated by the fourth harmonic of a Nd:YAG mode-locked laser. Due to the imperfections of the real components, the setup results in being, of course, far from an ideal event-ready source. But there is no apparent fundamental restriction for an improvement. The general conclusion of this study is that 3PDC-based setups are promising as deterministic or event-ready sources of biphotons.

II. THREE-PHOTON DOWN-CONVERSION PROCESS

A. Basic approach

The physics of 3PDC closely follows that of 2PDC, so that I review here only the main intermediate steps. I choose the crystal symmetry in such a way that the 2PDC process is absent. This is not really necessary, but it will presumably make the detection of the faint 3PDC fluorescence easier in practice. In the interaction picture and the parametric approximation, the Hamiltonian for 3PDC is then of the form

$$H = \sum h\omega_j(a_{jk}^\dagger a_{jk} + \tfrac{1}{2}) + \varepsilon_0 \int dV \chi^{(3)} E_p E_s^{(-)} E_i^{(-)} E_t^{(-)} + \text{H.c.}, \tag{3}$$

where $\chi^{(3)}$ is the third-order susceptibility tensor (it is considered a scalar constant here for simplicity). The three $E_j^{(-)}$ operators represent the quantified frequency down-converted fields [j can be s (signal), i (idler), t (trigger)]. The intense pump field E_p is assumed classical. This approximation is known to lead to a divergence in the number of signal photons, but it is acceptable for interaction times short enough or for negligible pump depletion [10]. A full-quantum description showing the deterministic generation of maximally entangled states in oscillators coupled through the third-order susceptibility has been reported very recently [11]. It is worth stressing that, in the same way as in 2PDC, the 3PDC fluorescence arises even in the absence of injected field. Following the usual approach [12] it is easy to see (in the limit $n_j \ll 1$) that the number of photons in the (for example) signal field (for one of the k modes) evolves as

$$n_s(t) = n_s(t=0)\cosh^2(st/2) + [1 + n_i(t=0)] \times [1 + n_t(t=0)]\sinh^2(st/2), \tag{4}$$

where s is proportional to $\chi^{(3)}E_p$. Therefore, even if all $n_j(t=0)=0$, there is a remaining term $\sinh^2(st/2) \approx (st/2)^2$ (the same as in the 2PDC case).

The "wave function" $|\Psi\rangle$ of the field at the exit surface of the crystal is calculated in the same way than for 2PDC. It results in being of the form [2]

$$|\Psi\rangle = |0\rangle + \sum F_{k,k',k''} a_{sk}^\dagger a_{ik'}^\dagger a_{tk''}^\dagger |0\rangle, \tag{5}$$

where the sum is performed over the two polarizations and all the possible wave vector values. The coefficient $F_{k,k',k''}$ in Eq. (5) includes the conditions of phase matching, and it is the result of the integration over time (from the first-order perturbation theory), the frequency spectrum (for pulsed pump beams [13]), and the volume of the crystal. The consequences of the finite size of the crystal and the pump field spectrum on the phase-matching conditions have been discussed in detail in several articles (for instance, Refs. [2,13]). In what follows I assume, for simplicity, that the perfect conditions for phase-matching hold:

$$\mathbf{k}_p = \mathbf{k}_s + \mathbf{k}_i + \mathbf{k}_t, \quad \omega_p = \omega_s + \omega_i + \omega_t. \tag{6}$$

This is equivalent to assuming a pulse with a narrow spectrum (relative to the central optical frequency), a crystal of infinite length, and neglect diffraction effects.

It has been known for a while that a three-body decay, as is apparently described by Eqs. (6), produces a poor level of entanglement [6]. However, inside a birefringent crystal the variation of the index of refraction with the direction of propagation imposes privileged directions of emission, given by the phase-matching conditions. When these conditions are taken into account $F_{k,k'.k''}$ is practically zero but for certain combinations of the ω_j and $\mathbf{k}_j$ and hence a state of the required form, Eq. (2), can be obtained. These privileged combinations are found in the next section.

B. Phase-matching conditions for 3PDC

Even for the collinear and degenerate process ($\mathbf{k}_s = \mathbf{k}_i = \mathbf{k}_t$, $\omega_s = \omega_i = \omega_t = \omega_p/3$), there are, in principle, several possible frequency down-conversion schemes or "cases": an ordinary photon that decays into three ordinary photons ($o \to o,o',o''$), into one extraordinary and two ordinary photons ($o \to o,o',e$), etc. Each case has different phase-matching conditions. In general, not all cases have realizable phase-matching conditions in a given material for a given wavelength. I restrict the study here to the case ($e \to o,o',e$) in a uniaxial crystal, for it will be useful for the example in Sec. IV. The phase-matching conditions for the other cases and for biaxial crystals are obtained according to the same approach and lead, essentially, to the same results.

The exact phase-matching conditions can be obtained only numerically [14]. However, approximate solutions valid for paraxial beams, small deviations from the collinear case and narrow spectra, lead to a physical picture easy to visualize, and they suffice for the purposes here. I follow the

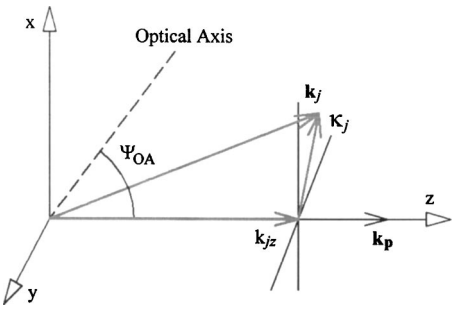

FIG. 1. Scheme of the wave vectors. The pump k_p is in the z direction. The optical axis of the (uniaxial) crystal is in the xz plane and forms an angle ψ_{OA} with the z axis. This angle is such that collinear phase matching for 3PDC holds. The vector $\mathbf{k}_j$ indicates the direction of emission of the frequency down-converted photon ($j=s,i,t$). Its projection on the z axis is k_{jz}, and its component in the xy plane is $\boldsymbol{\kappa}_j$. It is assumed that $|\boldsymbol{\kappa}_j/\mathbf{k}_j| \ll 1$—i.e., that the frequency down-converted photons are emitted at small angles from the pump direction.

approach and notation of Rubin's study of the 2PDC process [15]. Assume that the crystal has been cut so that, for a pump beam perpendicular to the crystal's face, collinear phase matching holds:

$$\Omega_e + \Omega_o + \Omega_{o'} = \omega_p, \quad (K_e + K_o + K_{o'}) \cdot \mathbf{e}_z = \mathbf{k}_p \cdot \mathbf{e}_z. \quad (7)$$

There are, in addition, other combinations of frequencies and wave numbers in the neighborhood of these values that are also phase matched. To see this, let us start by writing the expressions for the collinear wave numbers:

$$K_e = n_e(\Omega_e, \psi_{\mathrm{OA}})\Omega_e/c, \quad K_o = n_o(\Omega_o)\Omega_o/c, \quad (8)$$

where ψ_{OA} is the angle between the optical axis (which is assumed in the xz plane) and the z direction (see Fig. 1). The variables for the collinear phase matched condition are indicated with capital letters $\{\Omega, K\}$ and the ones for a noncollinear phase-matched condition with small letters $\{\omega, \mathbf{k}\}$. The differences between the noncollinear and collinear phase-matched frequencies are named $\nu_j = \omega_j - \Omega_j (|\nu_j| \ll \Omega_j)$. I choose "signal" to be the extraordinary beam, "idler" to be one of the ordinary beams, and "trigger" to be the remaining ordinary beam. I also choose that $K_i = K_t = K_o$, $\Omega_i = \Omega_t = \Omega_o$ (i.e., degenerate phase matching). Finally, $\boldsymbol{\kappa}_j$ denotes the component of the wave vectors in the xy plane, so that

$$\mathbf{k}_j = k_{jz}\mathbf{e}_z + \boldsymbol{\kappa}_j. \quad (9)$$

Taking into account these definitions, the phase-matching conditions, Eqs. (6), are now

$$k_p - k_{sz} - k_{iz} - k_{tz} = 0, \quad \nu_s + \nu_i + \nu_t = 0, \quad \boldsymbol{\kappa}_s + \boldsymbol{\kappa}_i + \boldsymbol{\kappa}_t = 0. \quad (10)$$

The values of the k_{jz} can be put in terms of K_j by taking into account the frequency change and the transverse displacement in an expansion at first order for ordinary rays,

$$k_{oz} = K_o + \nu_o/u_o - \kappa_o^2/(2K_o), \quad (11a)$$

while, for the extraordinary ray, there is an extra term coming from the variation of the index of refraction with the direction of propagation:

$$k_{sz} = K_s + \nu_s/u_s - \kappa_s^2/(2K_s) - N\boldsymbol{\kappa}_s \cdot \mathbf{e}_x, \quad (11b)$$

where $N = (1/n_e)\,\partial n_e/\partial \psi_{\mathrm{OA}}$ is the relative variation of the (extraordinary) index of refraction with the angle between the optical axis and the pump. In Eqs. (11a) and (11b), u_j is the group velocity: $1/u_j = d(\Omega_j n_j/c)/d\Omega_j$. As it is a first-order expansion, both N and u_j are calculated at the frequencies Ω_j. After replacement of Eqs. (11a) and (11b) into Eqs. (10) and taking into account Eqs. (7), the phase-matching condition reads

$$0 = \nu_s D + N\boldsymbol{\kappa}_s \cdot \mathbf{e}_x + \kappa_s^2/K - \boldsymbol{\kappa}_i \cdot \boldsymbol{\kappa}_t/K_o, \quad (12)$$

where $D \equiv 1/u_o - 1/u_e$ and $1/K \equiv \frac{1}{2}(1/K_o + 1/K_e)$. After eliminating (for example,) $\boldsymbol{\kappa}_i$ using the third equation of Eqs. (10), Eq. (12) reads

$$(\boldsymbol{\kappa}_s + \tfrac{1}{2}\mathbf{v})^2 = (\tfrac{1}{2}\mathbf{v})^2 - \nu_s DK - \eta\kappa_t^2 \equiv R^2, \quad (13)$$

where $\eta = K/K_o \approx 1$ and $\mathbf{v} \equiv NK\mathbf{e}_x + \eta\boldsymbol{\kappa}_t$. Equation (13) in the variable vector $\boldsymbol{\kappa}_s$ represents a circle (in the $\boldsymbol{\kappa}$ plane) of radius R centered on $-\frac{1}{2}\mathbf{v}$. All the s photons (simultaneously emitted with the t photon observed at $\boldsymbol{\kappa}_t$) are emitted on one of such circles. By using again the third of Eqs. (10), it is immediate to see that the phase matched values for $\boldsymbol{\kappa}_i$ lie also on a circle of radius R, but centered on $\frac{1}{2}\mathbf{v} - \boldsymbol{\kappa}_t$. Therefore, the simultaneously emitted i photon lies on such circle. Note that the value of the radius of the circles depends on ν_s, but not the position of their center.

In summary, let us suppose that we observe a "trigger" (t) photon at a certain angle given by $\boldsymbol{\kappa}_t$. Then, the s photon and the i photon (which are emitted simultaneously with the t photon) lie on two circles of the same radius. The value of the radius depends of the frequency of observation. But regardless of the value of the radius, due to the condition given by the third equation of Eqs. (10), the positions of the s and i photons are opposite through the symmetry point P (see Fig. 2). Note that this figure is similar to the one obtained for 2PDC, but as if the pump beam were at $-\frac{1}{2}\boldsymbol{\kappa}_t$.

III. PROPOSED EVENT-READY SOURCE

A. Sketch of the setup

The freedom to choose combinations for the phase matched $\boldsymbol{\kappa}_j$ and ν_j is again quite large. A simple possibility is to choose $\boldsymbol{\kappa}_t$ along the y axis. Then the figure is symmetric with respect to the y axis and also with respect to a "symmetry line" now passing at $-\frac{1}{2}\boldsymbol{\kappa}_t$ and parallel to the x axis (see Fig. 3). If an i photon (o polarized) is emitted on the left (right) of that symmetry line, then an s photon (e polarized) is emitted on the right (left). Now, the idea of the source is heuristically at hand. A mirror with a straight edge is placed just on that symmetry line, to split the left and right halves of the emitted field (see Fig. 4). Then each of the half-fields is focused on a single-mode optical fiber (or directly into the

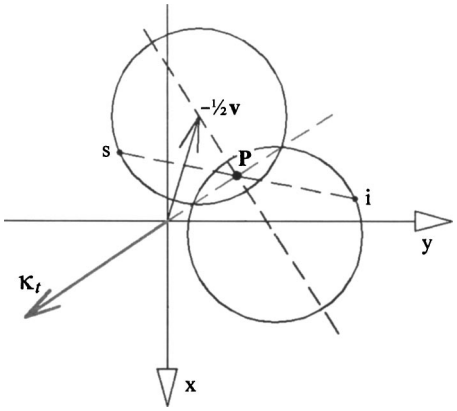

FIG. 2. Positions of phase matching in the $\boldsymbol{\kappa}$ plane. The pump beam is at the origin and propagates out of the page. If a trigger photon is detected at $\boldsymbol{\kappa}_t$, then the $\boldsymbol{\kappa}$ vector of the simultaneously generated signal *(s)* photon lies somewhere on a circle centered on $-\frac{1}{2}\mathbf{v}$ and the $\boldsymbol{\kappa}$-vector of the idler *(i)* photon lies on a conjugate circle of the same radius, centered at $\frac{1}{2}\mathbf{v}-\boldsymbol{\kappa}_t$. The line joining the *s* and *i* photons of the same pair passes through a point *P*, placed at $\frac{1}{2}\boldsymbol{\kappa}_t$, which is called the center of symmetry of the conjugated circles.

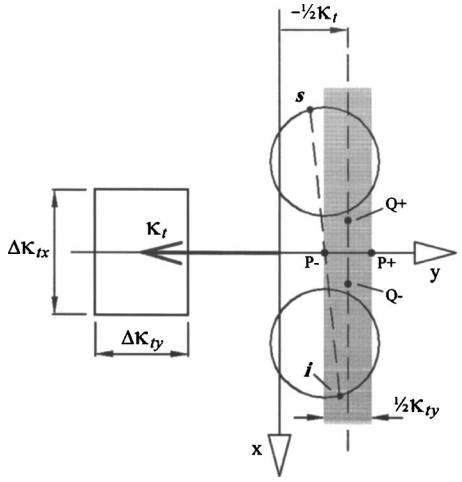

FIG. 3. Influence of the finite size of the detector for the trigger photon (the *t* detector). The area of the *t* detector in the $\boldsymbol{\kappa}$ plane is the rectangle on the left. The dotted vertical line at $-\frac{1}{2}\boldsymbol{\kappa}_t$ is the position of the splitting mirror. If the *t* photon is detected at the point $\boldsymbol{\kappa}_t+\frac{1}{2}\boldsymbol{\kappa}_{ty}$ (the point of the *t* detector closest to the origin), the corresponding *s* and *i* photons are emitted on conjugated circles whose center of symmetry is P^- ($\frac{1}{4}\Delta\boldsymbol{\kappa}_{\mathrm{ty}}$ to the left of the splitting mirror's line). As is seen in the figure, some pairs (like *s*, *i*) may fall on the same side of the splitting mirror's line and therefore they cannot produce simultaneous detections at *A* and *B* (see Fig. 4). The same happens with P^+. Instead, the conjugated circles with center of symmetry in Q^+, Q^- (which correspond to *t* photons detected at the top and bottom points of the *t* detector) are not laterally displaced from the splitting mirror's line and hence suffer no losses. The net effect of the size of the *t* detector is represented by the shadowed stripe (of "infinite" length in the *x* direction) of width $\frac{1}{2}\Delta\boldsymbol{\kappa}_{ty}$. Fluorescence falling inside this area cannot produce coincidences at *A* and *B* and must be considered lost. Note that the size of the detector in the *y* direction reduces the utilizable fluorescence, but not the size in the *x* direction, so that the best geometry for the detector has the shape of a thin slit parallel to the *x* axis.

detectors) at *A* and *B*. Any remaining information on the original direction of propagation of the photons is lost into the fibers (or in the detectors' surfaces), so that at the fibers' outputs there is no way to know if the detected photon is a (say) *i* photon (*o* polarized) coming from the circles centered on the lower side (of Fig. 3) or an *s* photon (*e* polarized) coming from the circles centered on the upper side. Recall that no spectral filtering is performed, so that the value of the radius of the circles is undetermined. In this way, in principle, all the *s* and *i* photons simultaneously emitted with the *t* photon are detected at *A* and *B*. Therefore, when a *t* photon is detected, one ideally has, with certainty, a biphoton available at *A* and *B*. A more formal deduction of this result is as follows:

The phase-matching conditions determine that the *o*-polarized photon detected at $\boldsymbol{\kappa}_t$ is created at the same time as the other two photons, *o* and *e* polarized. The frequency shifts ν_j and positions (in $\boldsymbol{\kappa}$ space) of these two photons are not determined. It is only known that if an *o(e)* photon is observed at $\boldsymbol{\kappa}$, then there is an *e(o)* photon observed at $-\boldsymbol{\kappa}-\boldsymbol{\kappa}_t$. As far as $\chi^{(3)}_{(\omega)}\approx$const(which is a good approximation as far as $\boldsymbol{\kappa}$ holds to the paraxial approximation), the state of the signal and idler photons is described then by

$$\int d\boldsymbol{\kappa}(|o,\boldsymbol{\kappa}\rangle|e,-\boldsymbol{\kappa}-\boldsymbol{\kappa}_t\rangle+|e,\boldsymbol{\kappa}\rangle|o,-\boldsymbol{\kappa}-\boldsymbol{\kappa}_t\rangle). \qquad (14)$$

The mirror splits this state into vectors "*a*" (i.e., having $\kappa_y+\frac{1}{2}\kappa_t<0$) and photons "*b*" $(\kappa_y+\frac{1}{2}\kappa_t>0)$, so that it is written now as

$$|\alpha\rangle\equiv(1/\sqrt{2})\int_{-\infty}^{+\infty}d\kappa_x\int_{-\infty}^{-\kappa_t/2}d\kappa_y(|o,\kappa_x,\kappa_y\rangle_a|e,-\kappa_x,-\kappa_y-\kappa_t\rangle_b$$
$$+|e,\kappa_x,\kappa_y\rangle_a|o,-\kappa_x,-\kappa_y-\kappa_t\rangle_b). \qquad (15)$$

The experimental setup is built in such a way that any other

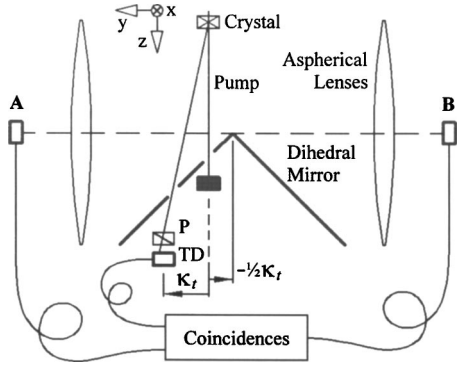

FIG. 4. Sketch of the proposed setup. A *t* photon with "*o*" polarization is selected with a polarizer (*P*) after passing through a thin slit (its larger side is parallel to the *x* axis). The right and left half-fields of Fig. 3 are separated with a dihedral mirror. Appropriate optics focus the photons on small-area detectors or single-mode optical fibers at *A* and *B*, where the information about their direction of propagation and frequency is lost.

information on the direction of propagation is lost. The corresponding state is then represented by the reduced density matrix

$$\int d\kappa_x' d\kappa_x'' d\kappa_y' d\kappa_y'' \langle \kappa_x'|_a \langle \kappa_x''|_b \langle \kappa_y'|_a \langle \kappa_y''|_b |\alpha\rangle \times \langle \alpha||\kappa_x'\rangle_a |\kappa_x''\rangle_b |\kappa_y'\rangle_a |\kappa_y''\rangle_b = \tfrac{1}{2}(|o\rangle_a|e\rangle_b + |e\rangle_a|o\rangle_b)(\langle o|_a\langle e|_b + \langle e|_a\langle o|_b), \quad (16)$$

which is the density matrix that corresponds to the Bell state $(1/\sqrt{2})$ $(|x,y\rangle+|y,x\rangle)$, and it is the result that was looked for.

The other states of the Bell's basis can be obtained by multiplying different regions in the $\boldsymbol{\kappa}$ integral with different phase factors. Physically, this is achieved by the insertion of wave plates and/or birefringent crystals into the optical paths [16].

It is immediate that the main limitation to this scheme comes from the practical difficulty of focusing the broad and divergent half-fields. If the collection efficiency is poor, there will be many failed triggers—i.e., an "event-ready" signal not followed by an entangled pair. However, if the pump beam is tightly focused on the crystal so that the fluorescence emerges from a pointlike source, it is possible, in principle, to collect all the emitted radiation even into a single-mode optical fiber.

Let us suppose that the collecting optics in Fig. 4 is made up of a pair of (commercially available) aspherical lenses with an f number of 0.6. Assuming that the fluorescence has a dipolelike intensity distribution with the shape of a $\cos^2$ lobe, these lenses collect roughly 55% of the total emitted radiation. If this radiation is to be efficiently inserted into a single-mode optical fiber (typically $\mathrm{N.A.}=0.1$, core radius 2.3 μm), the constant irradiance theorem indicates that the pumped area must have a radius of 0.35 μm. This value is attainable with a UV laser (for example, the fourth harmonic of Nd:YAG, $\lambda=266$ nm) with a good TEM_{00} beam quality.

Note that, despite the fact that 2PDC and 3PDC are similar processes, the setups and problems to solve are very different. In 2PDC, the pump beam is usually not focused into the crystal. Rather, the focusing optics is placed right before the crystal and in such a way that the radiation is focused into the detectors or fibers [17], which are far from the crystal to allow measuring the angles with precision. Besides, spectral filters select the entangled pair taking advantage of the angle-frequency correlations. In the proposed 3PDC setup instead, the pump is tightly focused into the crystal, and the collecting optics are (necessarily) close to the source. There is no spectral or angular filtering of the entangled photons, because one wants to collect all the photons emitted simultaneously with the trigger. The trigger is not filtered either, to destroy the frequency-angle correlation for the pair. Only its polarization (o, in this case) is selected.

Using aspherical lenses is the simplest choice, but any one of the devices used to collect incoherent radiation from small sources is an alternative: condenser mirrors (f number ≈ 0.33, which means a theoretical collecting efficiency of 84%), parabolic mirrors (f number ≈ 0.12, efficiency 99%), ellipsoidal cavities ($\approx$100% efficiency), or holograms [18].

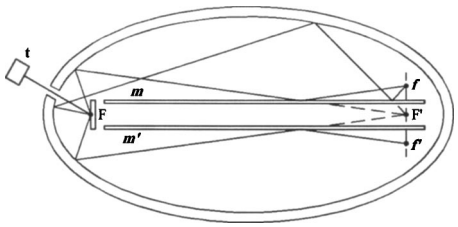

FIG. 5. Sketch of a possible setup with an ellipsoidal cavity, to improve the trigger's reliability ρ. The crystal is placed in the ellipsoid's focus F on the left. Part of the radiation leaves the cavity through a narrow slit (its larger dimension is perpendicular to the page) and goes into the t detector (the selecting polarizer is not indicated). The plane mirrors m, m' (which fully cover the ellipsoid's width perpendicular to the page) produce two images f and f' of the ellipsoid's focus F' on the right. The upper (left, in Fig. 4) and lower (right, in Fig. 4) half radiation fields are focused into f and f', respectively, where detectors or fiber focusing optics are placed. The pump beam (not drawn) propagates in the page and parallel to the ellipsoid's axis (not drawn, it joins F and F') at one-third of the distance between the axis and the slit for the trigger.

A sketch of a possible setup using an ellipsoidal cavity is shown in Fig. 5. The crystal is placed in one of the focuses of the ellipsoid. Two plane-parallel mirrors make two images of the other focus. The radiation emitted in the upper and the lower half of the ellipsoid is concentrated in each of these image points, where detectors or additional optics to focus into optical fibers are placed. In order to get rid of the scattered pumping UV radiation, the output face of the crystal should be high reflection (HR) coated and the ellipsoid's surface antireflection (AR) coated for the UV, and coated in the opposite way for the fluorescence spectral bandwidth.

An interesting variation of the setup is to choose the extraordinary photon as the trigger. If, once again, $\boldsymbol{\kappa}_t$ is chosen along the y axis, then the correlated s and i photons are emitted on the opposite sides of circles centered at $-\frac{1}{2}\boldsymbol{\kappa}_t$, like in 2PDC with phase-matching type I. As the entangled photons are both ordinary rays, there is no need for compensation of the dispersion and walk-off between signal and idler, which means a non-negligible experimental simplification. On the other hand, as they have the same and well-defined polarization, there is no entanglement in polarization. A polarization entangled state may be constructed by inserting a half-wave plate on the upper (or lower) half-fields.

B. Some practical limitations

One of the limitations of the proposed setup comes from the finite area of the detector for the trigger photon (the t detector). Assuming that it cannot act as a detector for the s and i photons too, its area must be subtracted from the collecting area. On the other hand, a small area implies a low rate of triggered biphotons. The largest rate is obtained when the area of the t detector is equal to one-half of the total collecting area. It is not possible to calculate the numbers for such a large area within the paraxial approximation. Besides, it is at first sight doubtful that a setup with such a large area for t can provide pure entangled states for s and i. In any

case, it is a subject that deserves a study with an approach not relying on the paraxial approximation.

Meanwhile, one can proceed within the paraxial approximation if the aim of reaching the maximum possible rate of triggered biphotons is given up. Assume then that the t detector has a small area, which is represented with a rectangle in the $\boldsymbol{\kappa}$ plane (Fig. 3). The fluorescence's symmetry point (which is P if the t photon is detected at the center of the t detector's area, $\boldsymbol{\kappa}_t$) shifts to P^-, P^+ if the t photon is detected at the horizontal extreme points in the detector's area $\boldsymbol{\kappa}_t \pm \Delta\boldsymbol{\kappa}_{ty}$ and to Q^-, Q^+ if the t photon is detected at the vertical extreme points in the detector's area $\boldsymbol{\kappa}_t \pm \Delta\boldsymbol{\kappa}_{tx}$ (recall that in Fig. 3 the x axis is in the vertical direction). Note now that, among the pairs simultaneously emitted with the t photon detected at $\boldsymbol{\kappa}_t + \Delta\boldsymbol{\kappa}_{ty}$, some of them, like (s,i), fall on the *same* side of the splitting mirror (which is physically centered on P, not on P^-, and is parallel to the x axis), and hence, they cannot produce a coincidence count between A and B (see Fig. 4). This deteriorates the trigger's reliability (that is, there is a trigger signal not followed by a detectable biphoton). Therefore, it is convenient to make $\Delta\boldsymbol{\kappa}_{ty}$ as small as possible. On the other hand, the effect of the finite size $\Delta\boldsymbol{\kappa}_{tx}$ of the detector on the direction x is merely to displace the center of symmetry from P to Q^+ and Q^-, but always on the symmetry line. As the fluorescence's symmetry line is not laterally shifted from the actual mirror's position, there are no "lost" pairs in this case.

Summarizing, the best choice for the geometry of the t detector is a thin slit in the direction y and with a length to the limit of the paraxial approximation in the direction x.

Now, let us look for a criterion for the best value of the modulus of $\boldsymbol{\kappa}_t$. From Eq. (13) the radius of the circles decreases if $\boldsymbol{\kappa}_t$ increases. Then, a larger value of $\boldsymbol{\kappa}_t$ makes the radiation easier to collect. But this criterion has some limits. One is given by the paraxial approximation on the value of $\boldsymbol{\kappa}_t/K$. The other one is that, for large $\boldsymbol{\kappa}_t$, the center of symmetry of the rings displaces rightwards (in Fig. 3), eventually into the region where the fluorescence intensity decays. As the bandwidth of the useful fluorescence is, at last, fatally limited by the optics, the detectors' spectral response, etc., a reasonable criterion seems to be to adjust the value of $\boldsymbol{\kappa}_t$ so that the collectable fluorescence fits to the bandwidth that is actually utilizable.

I take into account these criteria in the example in the next section.

IV. NUMERICAL EXAMPLE: CALCITE CRYSTAL PUMPED BY THE FOURTH HARMONIC OF Nd:YAG

A. Crystal

In choosing a material for 3PDC it seems convenient to look for a centrosymmetrical crystal, so that the second- order susceptibility tensor $\chi^{(2)}$ vanishes and, in consequence, also the 2PDC fluorescence, which may mask the radiation of interest. Another limitation comes from the necessity of a broad transmission range (at least from ω to 3ω). Of course, good bulk transparency, polishable surfaces, and resistance to focused laser beams must be also considered.

Calcite is a centrosymmetrical negative uniaxial crystal of the trigonal D_{3d} system [19]. It has been used in optics for more than one century. Optical technicians know well how to prepare calcite samples. It has been tested resistant to focused high-power pulsed lasers. It is less transparent to UV radiation and has a larger walk-off angle than some new crystals as, for example, α-BBO (do not confuse it with β-BBO). I have preferred calcite for this example because it is well known and, most important, because it is one of the materials used by Maker, Terhune, and Savage in their pioneering studies of "one-step" third-harmonic generation [20]. That experimental study provides valuable information, from which I have taken advantage of here. To begin, in Ref. [20] it is reported that the highest intensity of third-harmonic generation in calcite (thus, presumably, the highest value for the $\chi^{(3)}$ tensor) is obtained for the case

$$2 \text{ ordinary } (\omega) + 1 \text{ extraordinary } (\omega) \rightarrow 1 \text{ extraordinary } (3\omega).$$

That is why I choose the inverse process $(e \rightarrow o, o', e)$ for the description in Sec. III and in this example. The phase-matching angle for this process is found easily from the $n(\omega)$ curves for the material and the equation

$$2n_o(\omega) + n_e(\omega,\psi) = 3n_e(3\omega,\psi), \tag{17}$$

where $n_e(\omega,\psi) = \{\cos^2\psi/n_o^2(\omega) + \sin^2\psi/n_e^2(\omega)\}^{-1/2}$ and $n_o(\omega)$ and $n_e(\omega)$ are crystal constants given by Sellmeier's formulas. For calcite the formulas are (λ must be expressed in μm):

$$n_o^2 = 2.69705 + 0.0192064/(\lambda^2 - 0.01820) - 0.0151624\,\lambda^2, \tag{18}$$

$$n_e^2 = 2.18438 + 0.0082309/(\lambda^2 - 0.01018) - 0.0024411\,\lambda^2. \tag{19}$$

Then $n_e(798\text{ nm}) = 1.554$, $n_o(798\text{ nm}) = 1.648\,77$, and $n_e(266\text{ nm}) = 1.749\,69$. The phase-matching angle ψ turns out to be 46.95°. Note that this holds if the three frequency down-converted beams are collinear and have the same wavelength. One has the freedom to select them in a different way, perhaps more convenient than the one I analyze here.

Other parameters of interest are the $K_j = n_j 2\pi/\lambda : K_o = 12.9816\ 1/\mu\text{m}, K_e = 12.2357\ 1/\mu\text{m}$, and $K = 12.5977\ 1/\mu\text{m}$; then, $\eta \equiv K/K_o = 0.9703$. The group velocities are calculated from

$$u_j = (c/n_j)\{1 + (\lambda/n_j)dn_j/d\lambda\} \tag{20}$$

and [from Eq. (19)] $dn_o/d\lambda|_{798\text{ nm}} = -0.031\,631\ 1/\mu\text{m}$ and $dn_e/d\lambda|_{798\text{ nm}} = -0.013\,286\ 1/\mu\text{m}$, so that $u_o/c = 0.597\,23$ and $u_e/c = 0.639\,11$, and therefore $cD = 0.1097$. Finally,

$$N \equiv (1/n_e)\,\partial n_e/\partial\psi_{\text{OA}}|_{\lambda=798\text{ nm},\ \psi=46.95} = (1/n_e)\,\partial/\partial\psi\{\cos^2\psi/n_o^2 + \sin^2\psi/n_e^2\}^{-1/2} = -0.060346 \tag{21}$$

and all the necessary data are available now.

B. Estimation of the emission rate

I estimate the photon flux in 3PDC based on the observed photon flux in a 2PDC process. In an optimized 2PDC setup [21] a rate of 10^6 s^{-1} single counts is obtained on detectors with a measured efficiency of 0.286, which collect a 0.16° angle on a bandwidth of 4.3 nm. The 351-nm pumping laser delivers 300 mW of cw power, and it is focused to a spot with a radius of 82 μm into a β-BBO crystal 2 mm long. This means that, for an electric field into the crystal, $E_{(2\mathrm{PDC})} \approx 3.5\times 10^4$ V/m; the total emitted 2PDC flux is about 3×10^{12} s^{-1} ($\Delta\lambda/4.3$ nm), where $\Delta\lambda$ is the fluorescence bandwidth.

In order to scale these numbers to the 3PDC case, the correction factors are the different field intensities $(E_{(3\mathrm{PDC})}/E_{(2\mathrm{PDC})})^2$, then the different efficiencies of the 3PDC and 2PDC processes $(\chi^{(3)}E_{(3\mathrm{PDC})}/\chi^{(2)})^2$ and finally the different crystal lengths ($L_{crystal}$/2mm). In consequence,

$$N_{(3\mathrm{PDC})} \approx N_{(2\mathrm{PDC})}(E^4_{(3\mathrm{PDC})}/E^2_{(2\mathrm{PDC})})(\chi^{(3)}/\chi^{(2)})^2(L_{crystal}/2\ \mathrm{mm}). \tag{22}$$

In order to calculate the electric field for a cw pumping source (which corresponds to the 2PDC reference case), the energy inside the pumped volume is simply obtained by multiplying the nominal power of the laser (in W) with the time elapsed by the radiation to travel through the crystal, $\tau_{crystal}$. For a pulsed pumping source (the 3PDC example), the electric field is calculated using an "effective" value for the energy, which is obtained by multiplying the total pulse energy U with the ratio between the crystal length ($\approx\mu$m) and the pulse length ($L_{pulse}\approx$mm). The fluorescence is emitted only during the time $\tau_{crystal}$, so that the reference rate $N_{(2\mathrm{PDC})}$ must be multiplied with $\tau_{crystal}$ to get the correct reference number. Finally, to get the number of trios emitted per second, the number of crystal-crossing times during one pulse $(\tau_{pulse}/\tau_{crystal})$ and the number of pulses per second (C) must be taken into account:

$$N_{(3\mathrm{PDC})} \approx N_{(2\mathrm{PDC})}\tau_{crystal}(\chi^{(3)}/\chi^{(2)}E_{(2\mathrm{PDC})})^2 \times\left[\frac{U(L_{crystal}/L_{pulse})}{2\varepsilon_0 n^2\pi r^2 L_{crystal}}\right]^2\left(\frac{L_{crystal}}{2\ \mathrm{mm}}\right)(\tau_{pulse}/\tau_{crystal})C, \tag{23}$$

where $\varepsilon_0 = 8.85\times 10^{-12}$ A s/V m, n is the crystal's index of refraction, and r is the radius of the pumped volume. The effective length of the crystal is limited to the Rayleigh's length, $\pi r^2/\lambda$. The bandwidth $\Delta\lambda$ in the expression of $N_{(2\mathrm{PDC})}$ is limited by several factors. Considering the frequency shift for the maximum angle that can be collected with an aspherical lens with an f number of 0.6, $\Delta\lambda \approx 160$ nm, which is also nearly coincident with the efficiency bandwidth of silicon and the cutoff frequency of the assumed optical fiber. After simplifying several factors in Eq. (23), taking into account that for β-BBO $\chi^{(2)} = 1.6\times 10^{-12}$ m/V, using the data for 2PDC obtained above, and estimating (from the results in [20]) that $\chi^{(3)}_{\mathrm{calcite}} \approx 3\times 10^{-23}$ $(\mathrm{m/V})^2$, the expected 3PDC rate is

$$N_{(3\mathrm{PDC})} \approx 4\times 10^4\ U^2C/(L_{\mathrm{pulse}}r^2), \tag{24}$$

where the pulse energy is expressed in joules and the pulse length and pumped radius are expressed in meters.

There is an important difference with the 2PDC setup. In 2PDC, one would try to maximize Eq. (24) in order to get as many pairs per unit time as possible. If there were more than one pair inside the time observation window, one would reduce their number simply by adding spatial or spectral filtering. In 3PDC instead, one wants to collect *all* the pairs (i.e., for all propagation angles and frequencies) emitted simultaneously with the trigger photon. This forces that at most one trio must be *produced* at all frequencies and angles (instead of *observed* at a given angle and frequency) inside the time observation window (typically 3 ns, much longer than a mode-locking pulse). Otherwise, the correlation would be spoiled. In order to reduce the probability of producing two trios per pulse, down to a negligible level, the probability of producing one trio in a single pulse must be 10% or less. This means that $N_{(3\mathrm{PDC})} < 0.1C$. This imposes an upper limit to the acceptable pump power. In the previous section, the value of $r = 0.35$ μm has been obtained to allow focusing the fluorescence into a single mode fiber. Assuming pulses with a duration of 10 ps (usual for Nd:YAG mode-locked lasers) one finally gets

$$U < 30\ \mathrm{pJ}\ \text{or average power} < 3\ \mathrm{mW}\ (\text{for } C = 10^8\ \mathrm{s}^{-1}), \tag{25}$$

which is an accessible value for a standard diode-pumped mode-locked Nd:YAG laser, even for its fourth harmonic and with the requirement of a TEM_{00} beam. The 10-ns separation between successive pulses is usual in solid-state mode-locking lasers and allows a clear separation of the time observation windows.

Summarizing, with the described pump power and focusing, an average rate of 10^7 s^{-1} trios is predicted. Not all of them, however, can be used. A glimpse of what can be expected is obtained by assuming (as in [21]) a collecting area of 0.16° for the t detector. This means about 250 s^{-1} trigger counts. Assuming a 55% of collection efficiency (for the setup with the aspherical lenses), 75% for the detectors, and 95% for the coupling to the fibers, the probability that a biphoton is detected after the trigger (that is, the trigger's reliability, ρ) is

$$\rho = 0.55\times(0.75\times 0.95)^2 \approx 0.28. \tag{26}$$

(The collecting efficiency factor appears only once, because the signal and idler photons are emitted on circles of the same radius. If one of them is collected, the other one is also collected, with certainty.) Therefore, the expected rate of triggered biphotons is about 70 s^{-1}. This is poor if compared with the value of 10^5 s^{-1} of 2PDC [21], but it is favorable if compared with the 0.35 s^{-1} of a recent two 2PDC realization [22], and by sure it is much higher than what can be expected from the schemes of three 2PDC.

However, with only 70 s^{-1} effective counts, the typical dark count rate of the standard detectors (about 250 s^{-1}) produces a severe deterioration of the trigger's reliability. The influence of noise can be reduced by using selected (and more expensive) detectors with lower dark count rates or by using faster electronics and lower dispersion lines allowing narrower time observation windows, closer to the pulse duration. But probably the best available solution is simply to increase the number of trigger counts by enlarging the collecting angle of the *t* detector. Following the criteria discussed in Sec. III B, a slit detector 6.5 mm height and 0.1 mm wide placed at 33 mm (the focal distance of the assumed aspherical lens) of the crystal collects more than 10 times more radiation than the circular detector of 0.16° assumed in this example until now. With this slit-shaped *t* detector, about 10^3 s^{-1} trios and a trigger's reliability of 25% are expected, using noisy nonselected detectors and time observation windows of 3 ns duration with a separation of 10 ns.

V. SUMMARY

I have presented a study of the feasibility of using 3PDC as a deterministic or event-ready source of entangled states of photons. For a uniaxial crystal, the paraxial approach to the degenerate and collinear $e \rightarrow o, o', e$ case indicates that a structure of rings similar to the one observed in 2PDC is present, but with its center of symmetry displaced from the position of the pump beam, depending on the position the trigger photon observed. Also, depending if the trigger photon is an ordinary one or the extraordinary one, the structure of the rings is like that of 2PDC with phase-matching type II or I, respectively.

The proposed setup is based on the detection of a trigger photon and the collection of the largest part of the simultaneously emitted fluorescence, separating its left and right (from a certain symmetry line) halves, but otherwise losing any information about the angle of propagation and frequency of the signal and idler photons. In spite of the weakness of the third-order nonlinear term, the expected rate of entangled states is comparable to the one obtained in setups based on *two* 2PDC processes, and their purity is apparently free of fundamental limitations. Note that the total state generated by the proposed setup is of the form

$$|0\rangle + \xi\{\rho|t\rangle \otimes |\phi_{12}\rangle + (1-\rho)|t\rangle \otimes |\text{failed}\rangle + |\perp t\rangle \otimes \cdots\} + o(\xi^2), \tag{27}$$

where $|\text{failed}\rangle$ is a short way of indicating all the possibilities where the signal or the idler (or both) photons emitted simultaneously with $|t\rangle$ have not been detected. The purity of the state obtained after the observation of $|t\rangle$ hence depends on the value of the trigger's reliability (ρ), which is limited only by the instrumental imperfections, and the efficiency of 3PDC ξ, which can be made as small as required to make the last term in Eq. (27) negligible.

I have also found the phase-matching conditions for the calcite crystal and estimated the rate of triggered biphotons. Focusing the fourth harmonic of a (few mW average power) mode-locked Nd:YAG laser near to the diffraction limit, collecting the fluorescence with commercially available condenser optics and detecting with standard silicon avalanche photodiodes, the rate of triggered biphotons is estimated near 1000 s^{-1}, with a trigger's reliability of 25% (i.e., there are about 4000 s^{-1} trigger signals). These numbers can be doubled using more sophisticated collecting optics, as the ellipsoidal cavity sketched in Fig. 5.

In conclusion, this study indicates that the 3PDC process appears promising enough so as to proceed with an experimental attempt to measure the three-photon frequency downconversion fluorescence. On the theoretical side, the search for more convenient crystals and phase-matching conditions is probably the most necessary contribution. A study of the influence of the finite bandwidth of the trigger detector and a calculation of the phase-matching conditions free of the limitations of the paraxial approximation are also convenient.

ACKNOWLEDGMENTS

Many thanks to Professor Gregor Weihs (University of Vienna) for so many enlightening advices by email. Thanks also to Dr. Marcelo Kovalsky for a critical reading of the first version of this manuscript. This work was supported by Contract Nos. PIP 0425/98 (CONICET) and PICT99 03-06303 BID 1201 OC/AR (SEPCyT).

[1] P. Kok and S. Braunstein, Phys. Rev. A **62**, 064301 (2000).
[2] M. Rubin, D. Klyshko, Y. Shih, and A. Sergienko, Phys. Rev. A **50**, 5122 (1994).
[3] J. Clauser and M. Horne, Phys. Rev. D **10**, 526 (1974).
[4] G. Scalera, Lett. Nuovo Cimento Soc. Ital. Fis. **38**, 16 (1983).
[5] A. Hnilo, Found. Phys. **21**, 547 (1991).
[6] J. Clauser and A. Shimony, Rep. Prog. Phys. **41**, 1881 (1978).
[7] M. Zukowski, A. Zeilinger, M. Horne, and A. Ekert, Phys. Rev. Lett. **71**, 4287 (1993).
[8] J-W. Pan, M. Daniell, S. Gasparoni, G. Weihs, and A. Zeilinger, Phys. Rev. Lett. **86**, 4435 (2001).
[9] C. Sliwa and K. Banaszek, e-print: quant-ph/0207117, v2.
[10] M. Hillery, Phys. Rev. A **42**, 498 (1990).
[11] W. Leonski and A. Miranowicz, J. Opt. Soc. Am. B **6**, S37 (2004).
[12] A. Yariv, *Quantum Electronics*, 2nd ed. (Wiley, New York 1967).
[13] A. Joobeur, B. Saleh, and M. Teich, Phys. Rev. A **50**, 3349 (1994).
[14] G. Weihs, Ph.D. thesis, University of Vienna, 1999, pp. 139–145.
[15] M. H. Rubin, Phys. Rev. A **54**, 5349 (1996).
[16] P. Kwiat, K. Mattle, H. Weinfurter, A. Zeilinger, A. Sergienko, and Y. Shih, Phys. Rev. Lett. **75**, 4337 (1995).
[17] C. Monken, P. Souto Ribeiro, and S. Pádua, Phys. Rev. A **57**, R2267 (1998).

[18] G. Weihs (private communication).
[19] J. Nye, *Physical Properties of Crystals* (Oxford University Press, New York, 1957).
[20] P. Maker, R. Terhune, and M. Savage, *Proceedings of the Third Conference Quantum Electron* (Columbia University Press, New York, 1964).
[21] C. Kurtsiefer, M. Oberparleiter, and H. Weinfurter, Phys. Rev. A **64**, 023802 (2001).
[22] Z. Zhao, T. Yang, Y. Chen, A-N. Zhang, M. Zukowski, and J-W. Pan, Phys. Rev. Lett. **91**, 180401 (2003).